





## Destruction of surface states of $(d_{zx} + id_{yz})$ -wave superconductor by surface roughness: Application to $\text{Sr}_2\text{RuO}_4$

Shu-Ichiro Suzuki <sup>1,\*</sup>, Satoshi Ikegaya <sup>2</sup>, and Alexander A. Golubov <sup>1</sup>

<sup>1</sup>MESA+ Institute for Nanotechnology, University of Twente, 7500 AE Enschede, The Netherlands

<sup>2</sup>Department of Applied Physics, Nagoya University, Nagoya 464-8603, Japan

 (Received 8 July 2022; revised 27 September 2022; accepted 29 September 2022; published 1 November 2022)

The fragility of the chiral surface current of the  $(d_{zx} + id_{yz})$ -wave superconductor, a potential candidate for  $\text{Sr}_2\text{RuO}_4$  against surface roughness is demonstrated utilizing the quasiclassical Eilenberger theory. Comparing the chiral surface currents of  $(d_{zx} + id_{yz})$ -wave and  $(p_x + ip_y)$ -wave pairings, we conclude the chiral current for  $(d_{zx} + id_{yz})$ -wave SC is much more fragile than that for the  $(p_x + ip_y)$ -wave one. The difference can be understood in terms of the orbital symmetry of the odd-frequency Cooper pairs arising at the surface. Our results show the  $(d_{zx} + id_{yz})$ -wave scenario can explain the null spontaneous magnetization in  $\text{Sr}_2\text{RuO}_4$  experiments.

DOI: [10.1103/PhysRevResearch.4.L042020](https://doi.org/10.1103/PhysRevResearch.4.L042020)

**Introduction.** The determination of the pairing symmetry in  $\text{Sr}_2\text{RuO}_4$  (SRO) superconductors (SCs) has been an unsolved problem for more than a quarter century [1–4]. In the past few years, nevertheless, researchers in this field undergo a remarkable paradigms shift. Specifically, recent precise experiments on spin susceptibility [5–8] appear to contradict a spin-triplet odd-parity superconducting state with broken time-reversal symmetry (TRS) [9], which had, heretofore, been the leading candidate in SRO. Alternatively, an exotic *inter-orbital-singlet* spin-triplet even-parity state with broken time-reversal symmetry has come under the spotlight [10,11] because it can explain recent two remarkable experimental observations, i.e., a sharp jump in the shear elastic constant  $c_{66}$  at the superconducting transition temperature measured by ultrasound experiments [12,13], and a stress-induced split between the onset temperatures for the superconducting state and broken TRS state measured by muon spin-relaxation experiments ( $\mu\text{SR}$ ) [14,15]. Nowadays, careful and intensive verification for the realization of the interorbital superconducting state in SRO has been underway.

On the basis of a microscopic model for the interorbital superconducting state of SRO [10], the superconducting gap on the three Fermi surfaces of SRO has a  $(d_{zx} + id_{yz})$ -wave pairing symmetry [i.e.,  $(d + id')$ -wave SC]. It has been shown that the  $(d + id')$ -wave SC hosts characteristic surface states [16–19]. At material surfaces parallel to the  $z$  axis (i.e., the  $c$  axis of the SRO), the  $(d + id')$ -wave SC exhibits dispersing chiral surface states due to the chiral pairing symmetry with fixed  $k_z$ . Moreover, the pure odd-parity nature with respect to  $k_z$  results in the emergence of dispersionless zero-

energy surface states at the surfaces perpendicular to the  $z$  axis. Thus, observations of these surface states can be the conclusive evidence for the interband superconducting state in SRO. However, scanning superconducting quantum interference devise experiments [20,21] have not detected the expected spontaneous edge current due to the chiral surface states [22–28], and tunneling spectroscopy measurements along the  $z$  axis did not observe a zero-bias conductance peak suggesting the dispersionless zero-energy surface states [29–31]. Therefore, when we take the experimental observations at face value, the interorbital superconducting state with a  $(d + id')$ -wave superconducting gap seems to be excluded.

In this Letter, we study the influence of surface roughness on the surface states of the  $(d + id')$ -wave SC. The most straightforward numerical simulation is adding random potentials to the microscopic three-orbital Hamiltonian [10]. However, such numerical simulation requires significantly large systems in real space, ensemble averaged of impurity configurations, and self-consistent treatments for the order parameter, meaning that it would be impossible to implement owing to the prohibitive numerical costs. Alternatively, we employ the quasiclassical Eilenberger theory for a simple single band and clarify essential properties of the surface states of the  $(d + id')$ -wave SC. As a result, we demonstrate that the surface current due to the chiral surface states and the sharp zero-energy peak in the surface density of states due to the dispersionless zero-energy surface states are easily destroyed by surface roughness. Importantly, the vulnerability of the surface states is owing to a roughness-induced destructive interference effect which is inevitable with the  $(d + id')$ -wave pairing symmetry. Namely, the surface states of the  $(d + id')$ -wave SC in the presence of surface roughness are fragile regardless of details of the model.

In actual experiments, a surface is not as ideal as in theoretical models. The electronic structure near a surface must be modified by the damaged or deformed crystal structure. Since the surface states of a  $(d + id')$ -wave SC are shown to be fragile, it is essential to pay attention to the surface quality

\*s.suzuki-1@utwente.nl

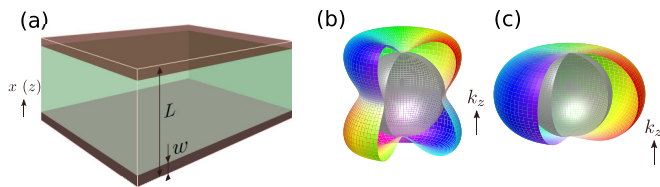


FIG. 1. (a) Schematics of the system. The surfaces are parallel to either the  $x$  or  $z$  axis. The widths of the superconductor and disordered regions are denoted by  $L$  and  $w$ . The translational symmetry is assumed in the direction parallel to the surfaces. The pair potentials of  $(d_x + id_y)$ - and  $(p_x + ip_y)$ -wave superconductors are shown in (b) and (c). The color indicates  $\arg[\Delta(k)]$ . The inner silver sphere represents the Fermi sphere.

of a sample to observe surface-state signatures. Therefore, we will conclude that the absence of surface-state signatures does not straightforwardly deny the realization of  $(d + id')$ -wave superconducting states.

*Quasiclassical Eilenberger theory.* We examine the effects of surface roughness utilizing the quasiclassical Eilenberger theory [32]. This approximation allows us to extract the essential spatial profile (i.e., coherence-length order) from the Green's function by ignoring the rapid oscillation with the Fermi-wavelength order. The SC has a pair of parallel surfaces which are perpendicular to the  $x$  or  $z$  axis as shown in Fig. 1(a). The thin dirty layers with the width  $w$  are introduced. The Green's functions obey the Eilenberger equation [33],

$$iv_F \cdot \nabla \check{g} + [i\omega_n \check{\tau}_3 + \check{H}, \check{g}]_- = 0, \quad (1)$$

$$\check{H} = \check{\Delta} + \check{\Sigma} = \begin{pmatrix} \check{\xi} & \check{\eta} \\ \check{\eta} & \check{\xi} \end{pmatrix}, \quad \check{\Sigma} = \frac{i}{2\tau_0} \langle \check{g} \rangle, \quad (2)$$

$$\check{g} = \begin{pmatrix} \check{g} & \check{f} \\ -\check{f} & -\check{g} \end{pmatrix}, \quad \check{\Delta} = \begin{pmatrix} 0 & \hat{\Delta} \\ \hat{\Delta} & 0 \end{pmatrix}, \quad (3)$$

where  $\langle \dots \rangle = \int_0^\pi \int_{-\pi}^\pi \dots \sin \theta d\varphi d\theta / 4\pi$ ,  $\check{g} = \check{g}(\mathbf{r}, \mathbf{k}, i\omega_n)$  is the quasiclassical Green's function in the Matsubara representation,  $\hat{\Delta} = \hat{\Delta}(\mathbf{r}, \mathbf{k})$  is the pair-potential matrix,  $\check{\Sigma} = \check{\Sigma}(\mathbf{r}, i\omega_n)$  is the self-energies by the impurity scatterings, and we assume the system is in equilibrium. The mean free path is denoted  $\ell = v_F \tau_0$  with  $\tau_0$  being the mean free time that is fixed at a certain value in the disordered region but infinitely large in the other place. In this Letter, the accents  $\check{\cdot}$  and  $\hat{\cdot}$  mean matrices in particle-hole and spin space. The identity matrices in particle-hole and spin space are, respectively, denoted by  $\check{\tau}_0$  and  $\hat{\sigma}_0$ . The Pauli matrices are denoted by  $\check{\tau}_j$  and  $\hat{\sigma}_j$  with  $j \in 1-3$ . All of the functions satisfy the symmetry relation  $\hat{K}(\mathbf{r}, \mathbf{k}, i\omega_n) = [\hat{K}(\mathbf{r}, -\mathbf{k}, i\omega_n)]^*$ , where the unit vector  $\mathbf{k}$  represents the direction of the Fermi momentum. Effects of the vector potential are ignored because it affects on surface states only quantitatively. We did not introduce a potential between the clean and disordered regions because this is not a physical boundary.

The Eilenberger equation (1) can be simplified by the so-called Riccati parametrization [34–36]. The Green's function

can be expressed in terms of the coherence function  $\hat{\gamma} = \hat{\gamma}(\mathbf{r}, \mathbf{k}, i\omega_n)$ ,

$$\check{g} = 2 \begin{pmatrix} \hat{\mathcal{G}} & \hat{\mathcal{F}} \\ -\hat{\mathcal{F}} & -\hat{\mathcal{G}} \end{pmatrix} - \check{\tau}_3, \quad (4)$$

$$\hat{\mathcal{G}} = (1 - \hat{\gamma} \hat{\gamma})^{-1}, \quad \hat{\mathcal{F}} = (1 - \hat{\gamma} \hat{\gamma})^{-1} \hat{\gamma}. \quad (5)$$

The equation for  $\hat{\gamma}$  is given by

$$(iv_F \cdot \nabla + 2i\omega_n) \hat{\gamma} + \hat{\xi} \hat{\gamma} - \hat{\gamma} \hat{\xi} - \hat{\eta} + \hat{\gamma} \hat{\eta} \hat{\gamma} = 0. \quad (6)$$

Assuming no spin-dependent potential and single-spin  $\hat{\Delta}$ , we can parametrize the spin structure of the functions,

$$\hat{\Delta} = i\Delta_{k,\nu}(i\hat{\sigma}_\nu \hat{\sigma}_2), \quad (7)$$

$$\hat{\Delta} = -i\Delta_{-k,\nu}^*(i\hat{\sigma}_\nu \hat{\sigma}_2)^* = i\Delta_{k,\nu}^*(i\hat{\sigma}_\nu \hat{\sigma}_2)^\dagger, \quad (8)$$

$$\hat{g} = g\hat{\sigma}_0, \quad \hat{f} = f_\nu(i\hat{\sigma}_\nu \hat{\sigma}_2), \quad \hat{f} = \underline{f}_\nu(i\hat{\sigma}_\nu \hat{\sigma}_2)^\dagger, \quad (9)$$

$$\hat{\eta} = i\eta_\nu(i\hat{\sigma}_\nu \hat{\sigma}_2), \quad \hat{\eta} = i\underline{\eta}_\nu(i\hat{\sigma}_\nu \hat{\sigma}_2)^\dagger, \quad (10)$$

where  $\nu = 0$  ( $\nu \in \{1-3\}$ ) is for the spin-singlet (spin-triplet) SC. In the following, we make  $\nu$  explicit only when necessary. Equation (6) can be reduced to

$$v_F \cdot \nabla \gamma + 2\tilde{\omega} \gamma - \eta + \eta \gamma^2 = 0, \quad (11)$$

$$\tilde{\omega} = \omega_n + \frac{\text{Re}\langle g \rangle}{2\tau_0}, \quad (12)$$

$$\eta_\nu = \Delta_k + \frac{\langle f \rangle}{2\tau_0}, \quad \underline{\eta}_\nu = \Delta_k^* - S_\nu \frac{\langle f \rangle^*}{2\tau_0}. \quad (13)$$

The coherence functions in the homogeneous limit  $\bar{\gamma}$  is given by

$$\bar{\gamma}(\mathbf{k}, i\omega_n) = \frac{s_o \Delta_k}{|\omega_n| + \sqrt{\omega_n^2 + |\Delta_k|^2}}, \quad (14)$$

with  $s_o = \text{sgn}[\omega_n]$  and  $\bar{\cdot}$  means the bulk value.

The momentum dependence of the pair potential is assumed as

$$\Delta_k = \begin{cases} 2(\Delta_1 k_x + i\Delta_2 k_y)k_z & \text{for the } (d + id') \text{ wave,} \\ \Delta_1 k_x + i\Delta_2 k_y & \text{for the } (p + ip') \text{ wave,} \end{cases} \quad (15)$$

where we put the factor 2 in the  $(d + id')$ -wave case such that  $\max[\Delta_k] = \bar{\Delta}$  in the homogeneous limit. The schematic gap amplitudes in the bulk are shown in Figs. 1(b) and 1(c) where the color means the phase of the pair potential  $\arg[\Delta(\mathbf{k})]$ . The spatial dependence of the pair potentials are determined by the self-consistent gap equation which relates  $f$  and  $\Delta$ ,

$$\Delta_\mu(\mathbf{r}) = 2\lambda N_0 \frac{\pi}{i\beta} \sum_{\omega_n}^{s_c} \langle V_\mu(\mathbf{k}') f(\mathbf{r}, \mathbf{k}', i\omega_n) \rangle, \quad (16)$$

$$\lambda = \frac{1}{2N_0} \left[ \ln \frac{T}{T_c} + \sum_{n=0}^{n_c} \frac{1}{n + 1/2} \right]^{-1}, \quad (17)$$

where  $\mu = 1$  or 2,  $\beta = 1/T$ ,  $T_c$  is the critical temperature,  $N_0$  is the density of the states (DOS) in the normal state at the Fermi energy, and  $n_c$  is the cutoff integer. The corresponding

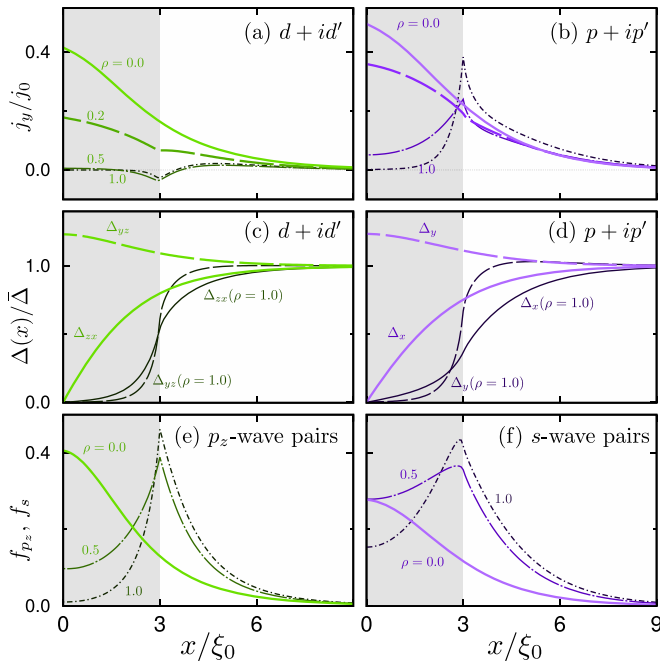


FIG. 2. Calculated results for the (a), (c), and (e)  $(d + id')$ -wave and (b), (d), and (f)  $(p + ip')$ -wave SCs. (a) and (b) The edge-current density in the  $y$  direction, (c) and (d) self-consistent pair potentials  $\Delta$ , and (e) and (f) subdominant pair amplitudes are shown. The surface-roughness parameters are fixed as  $\rho = \xi_0/\ell$  and  $w = 3\xi_0$ . The current density is normalized to  $j_0 = |e|v_F N_0 \pi T_c$ .

attractive potentials are  $(V_1, V_2) = (15/2)(k_z k_x, k_y k_z)$  for the  $(d + id')$ -wave and  $(V_1, V_2) = 3(k_x, k_y)$  for the  $(p + ip')$ -wave SCs.

The charge current, local DOS, and angle-resolved DOS are calculated from the Green's function,

$$j_y(\mathbf{r}) = eN_0 \frac{\pi}{i\beta} \sum_{\omega_n} \langle k_y \text{Tr}[\check{\tau}_3 \check{g}(\mathbf{r}, \mathbf{k}, i\omega_n)] \rangle, \quad (18)$$

$$N(\mathbf{r}, E) = \int N_{\text{AR}}(\mathbf{r}, k_y, E) dk_{\parallel}, \quad (19)$$

$$\frac{N_{\text{AR}}}{N_0} = \sum_{\alpha=\pm 1} \text{Re}[g(\mathbf{r}, \pm k_{\perp}, \mathbf{k}_{\parallel}, i\omega_n)]_{i\omega_n \rightarrow E+i\delta}, \quad (20)$$

where  $e < 0$  is the charge of an electron,  $\mathbf{k}_{\parallel}$  ( $k_{\perp}$ ) is the momentum parallel (perpendicular) to the surface. The amplitude of the subdominant Cooper pairs can be extracted from the anomalous Green's function,

$$f_{p_z} = \langle k_z f \rangle, \quad f_s = \langle f \rangle, \quad (21)$$

In the numerical simulations, we fix the parameters:  $L = 80\xi_0$ ,  $w = 3\xi_0$ ,  $\omega_c = 10\pi T_c$ ,  $T = 0.2T_c$ , and  $\delta = 0.01\bar{\Delta}$  with  $\xi_0 = \hbar v_F / 2\pi T_c$  being the coherence length.

**Chiral surface current and pair functions.** We first discuss the result for the open surface in the  $x$ -axis direction. The spatial profiles of  $j_y$  and  $\Delta$  are shown in Figs. 2(a)–2(d) where the results for the  $(d + id')$ -wave and  $(p + ip')$ -wave SCs are shown in the left and right panels, respectively. Figures 2(a) and 2(b) show the chiral surface current (CSC) for the  $(d + id')$ -wave SC is much more sensitive to the surface roughness than the  $(p + ip')$ -wave case. Even with a weak surface

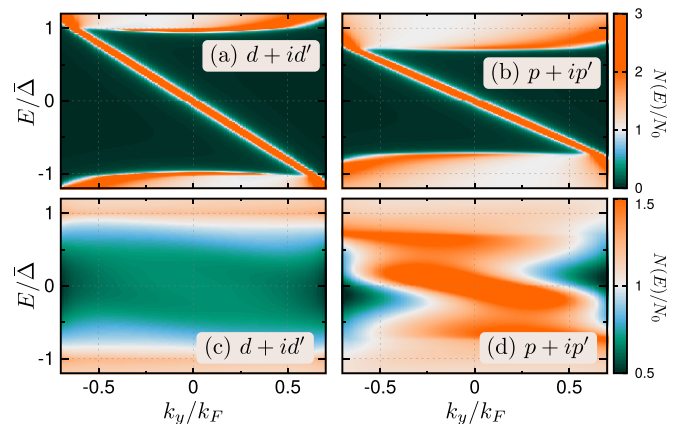


FIG. 3. Angle-resolved density of states at  $k_z/k_F = 1/\sqrt{2}$  for the (a) and (c)  $(d + id')$ -wave and (b) and (d)  $(p + ip')$ -wave SCs. The results are obtained at  $x = 0$  for the clean case [(a) and (b)] and at  $x = w$  for the rough case with  $\xi_0/\ell = 0.5$  [(c) and (d)]. The ARDOS are normalized to its value in the normal state.

roughness (i.e.,  $\xi_0/\ell = 0.5$ ), the CSC for the  $(d + id')$ -wave SC is almost zero [37], whereas that for the  $(p + ip')$ -wave SC is sufficiently large to be observed [26–28] where the peak in the current density moves from the surface to the internal surface between the disordered and ballistic regions. The pair potentials for the both SCs show qualitatively the same behavior to the surface roughness. At the clean surface, the component that changes its sign during the reflection (i.e.,  $\Delta_{zx}$  and  $\Delta_x$ ) becomes zero as shown in Figs. 2(c) and 2(d). Correspondingly, the other component is enhanced. When the surface is rough, both of the components are strongly suppressed due to the random scatterings.

The difference in the robustness of the CSC comes from the symmetry of the subdominant Cooper pairs induced by the local inversion-symmetry breaking at a surface. The inversion-symmetry breaking results in the parity mixing of the pair amplitudes [38]. Namely, odd-parity [even-parity] pairings are induced at a surface of the  $(d + id')$ -wave [ $(p + ip')$ -wave] SC. The  $p_z$ - and  $s$ -wave pair amplitudes (i.e., subdominant pairs with the lowest azimuthal quantum number) in each SC are shown in Figs. 2(e) and 2(f) where we fix  $\omega_n = \omega_0$ . The  $s$ -wave subdominant pairs plays an important role under a disordered potential, whereas the  $p_z$  wave does not. The  $s$ -wave pairs ( $f$ ) act as an effective pair potential in a disordered region [See Eq. (13)]. Namely, the disordered region of the  $(p + ip')$ -wave SC becomes an effective  $s$ -wave SC rather than a normal metal. Consequently, the chiral current of the  $(p + ip')$ -wave SC flows along the internal interface at  $x = w$ . In the Appendix, we show that  $\check{g}$  at the internal interface is qualitatively the same as that at a surface of a  $p$ -wave SC. The chiral current does not flow at the internal interface in  $(d + id')$ -wave cases because the anisotropic  $p_z$ -wave pairs cannot act as an effective pair potential [i.e.,  $\langle f \rangle = 0$  in Eq. (13)].

The angle-resolved DOS (ARDOS) for the  $(d + id')$ - and  $(p + ip')$ -wave SCs are compared in Fig. 3 where we fix  $k_z = k_F/\sqrt{2}$ . The ARDOS with  $\rho = 0$  ( $\rho = 0.5$ ) are obtained at the surface (internal interface). In the clean limit, the chiral surface states are prominent in each SC. When the surface

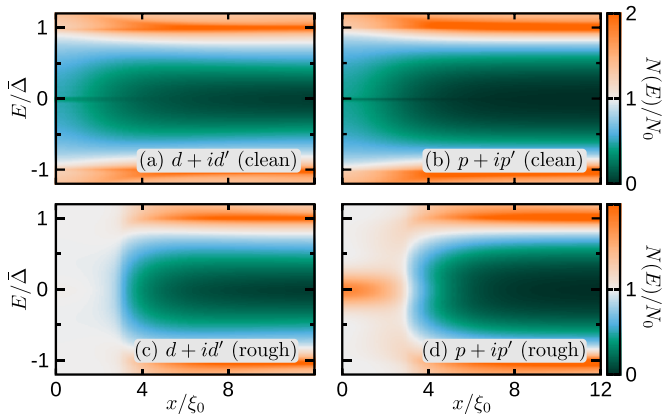


FIG. 4. Local density of states of the (a) and (c)  $(d + id')$ -wave and (b) and (d)  $(p + ip')$ -wave SCs. The surface roughness is set to  $\xi_0/\ell = 0.5$  and  $w = 3\xi_0$  in (c) and (d). The LDOS at  $x = 0$  is enhanced because of the chiral surface states. In  $(d + id')$ -wave case, the disordered region can be regarded as a normal metal [i.e.,  $N(E) = N_0$ ]. The LDOS is normalized to its value in the normal state  $N_0$ .

is rough, the chiral states for the  $(d + id')$ -wave SC vanishes [Fig. 3(c)], whereas that for the  $(p + ip')$ -wave SC is robust [Fig. 3(d)]. The local density of states (LDOS) can be calculated by integrating ARDOS. The results are shown in Fig. 4. We see the chiral surface states appear at the surface; the LDOS increases at the surface (light blue region) as shown in Figs. 4(a) and 4(b). Under the surface roughness,  $N(x, E) = N_0$  in the disordered region of the  $(d + id')$ -wave case, meaning that the disordered region becomes a normal metal. In the  $(p + ip')$ -wave SC, on the contrary, the LDOS has a peak structure in the disordered region, reflecting the emergence of the effective  $s$ -wave superconductivity in the disordered region. To detect the chiral surface states of the  $(d + id')$ -wave SC, one has to pay close attention to the surface quality because they are very sensitive to the roughness.

*Andreev bound states at the  $c$ -axis surface.* At the surface in the  $c$ -axis direction of the  $(d + id')$ -wave SC, the dispersion-less zero-energy states (ZESs) appear [16–18]. The effects of the surface roughness are shown in Fig. 5 where we also show the results for a  $p_z$ -wave SC (i.e., polar state with  $\Delta_k \sim p_z$ ) as a reference [39]. The ZESs for both SCs are prominent in the clean limit [Figs. 5(a) and 5(d)]. However, in the  $(d + id')$ -wave case, the ZESs become broader even by weak surface roughness (e.g.,  $\xi_0/\ell = 0.2$ ). Contrary to the  $p_z$ -wave SC [40–42], the ZESs of the  $(d + id')$ -wave SC disappear even for the weak disorder (i.e.,  $\xi_0 < \ell$ ).

The fragility of the ZESs can be explained by the absence of the  $s$ -wave subdominant pairs  $\langle f \rangle$ . The  $p_z$ -wave SC has robust ZESs supported by the  $s$ -wave pairs [41] (i.e., effective pair potential). On the other hand, the subdominant pairs for the  $(d + id')$ -wave SC are  $(p_x + ip_y)$ -wave-like pairs because of the phase winding at a fixed  $k_z$ . Anisotropic  $(p_x + ip_y)$ -wave pairs do not act as an effective pair potential [i.e.,  $\langle f \rangle = 0$  in Eq. (13)]. Therefore, the ZES at a surface in the  $c$ -axis direction of a  $(d + id')$ -wave SC are fragile against roughness.

*Discussion.* The important factor determining the robustness of surface states is only the presence of subdominant

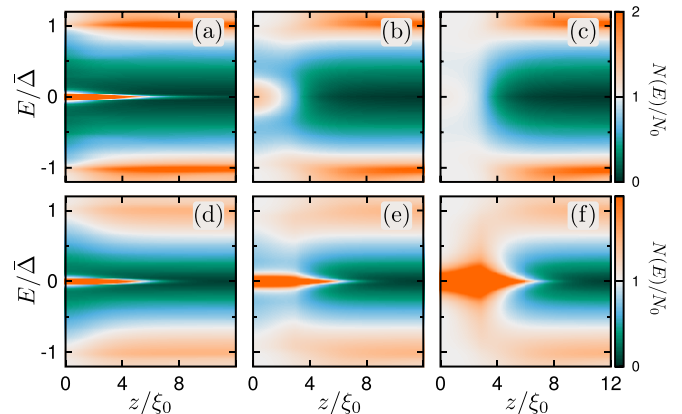


FIG. 5. Effects of the surface roughness on the dispersionless surface states of (a)–(c) the  $(d + id')$ -wave and (d)–(f)  $p_z$ -wave SCs. The surface is perpendicular to the  $z$  axis. The strength of the roughness is set to (a) and (d)  $\xi_0/\ell = 0.0$ , (b) and (e) 0.2, and (c) and (f) 0.5. The results are obtained from the self-consistent  $\Delta$  (not shown). The surface state in the  $z$  direction of the  $(d + id')$ -wave case is much more fragile than those of  $p_z$ -wave case.

$s$ -wave pairing induced at a surface. Therefore, we can generalize our knowledge to higher-order chiral superconductors. We have confirmed that the chiral surface states of  $(f_{x(5z^2-1)} + if'_{y(5z^2-1)})$ -wave SC are fragile against roughness because the  $s$ -wave pairs have a small amplitude. Similarly, we can anticipate fragile dispersionless ZESs in the  $(f_{(x^2-y^2)z} + if_{xyz})$ -wave SC since no  $s$ -wave pairing is expected.

In this Letter, we employ the simple single-band model and ignore the multi-orbital nature of SRO. The fragility of the surface states is owing to the absence of  $s$ -wave Cooper pairs at the surface. In a  $(d + id)$ -wave SC, such  $s$ -wave subdominant pairs can be induced only in extreme cases: The scatterings by roughness cause a constructive interference for  $s$ -wave pairs. Therefore, the fragility of the surface states of the  $(d + id')$ -wave SC would be irrelevant to the details of the model. Studying the roughness effects in detail with more realistic three-orbital models [10] would be an important future task where the surface states would be suffered additionally from more complicated interband scatterings.

We also mention that there are several remaining contradictions in the experimental findings. A recent Josephson current measurement suggests time-reversal invariant superconductivity in SRO [43] [and, thus, contradicts with the TSR-breaking  $(d + id')$ -wave states], whereas broken TRS has been observed in the  $\mu$ SR [14,15] and Kerr-rotation experiments [44]. In addition, a recent specific heat measurement under the strain [45] seems to contradict the two-component superconducting states [46] [and, therefore, the  $(d + id')$ -wave states], whereas the two-component superconducting states are supported by the recent ultrasound [12,13] and  $\mu$ SR experiments under the strain. Resolving these puzzles, which may be achieved by future microscopic studies providing alternative interpretations for the experimental data, would be important future tasks. However, they are beyond the scope of this Letter.

The surface-related phenomena in SRO has been clarified gradually. A recent experiment reported the magnetization

in the *normal state* due to the deformed crystal structure at the (001) surface [47], meaning that the electronic structure is locally modified near the surface. Reflecting the surface modification, the superconducting state may be reconstructed locally; the pairing symmetry at a surface can be different from that in the bulk. This is another possibility that the surface-state signature has not been observed. The relation among the surface magnetization, pairing symmetry at a surface, and the TRS-breaking superconductivity would be an interesting topic.

*Conclusion.* We have investigated the effects of surface roughness on the surface states of the  $(d_{zx} + id_{yz})$ -wave SC. Utilizing the quasiclassical Eilenberger theory, we have demonstrated that the surface states of the  $(d_{zx} + id_{yz})$ -wave SC are easily destroyed by surface roughness. Since the surface roughness is inevitable in real-life experiments, the absence of the experimental signatures from the surface states [20,21,29–31] would not be clearly inconsistent with the interorbital  $(d_{zx} + id_{yz})$ -wave superconducting state in SRO [10].

*Acknowledgments.* We are grateful to A. Brinkman, Y. Asano, and T. Kokkeler for the fruitful discussions. S.-I. S. is supported by JSPS Postdoctoral Fellowship for Overseas Researchers and a Grant-in-Aid for JSPS Fellows (JSPS KAKENHI Grant No. JP19J02005), and thanks the University of Twente for hospitality. S.I. was supported by a Grant-in-Aid for JSPS Fellows (JSPS KAKENHI Grant No. JP21J00041).

#### APPENDIX: EFFECTS OF SELF-ENERGY IN A DIRTY NORMAL METAL ATTACHED TO A $p$ -WAVE SC

In this section, we consider a simplified theoretical model: The interface between a dirty normal metal (DN) and a  $p$ -wave SC. For simplicity, we ignore the spatial dependence of the Green's functions near the interface. The Riccati

equations in the DN and SC are

$$\mathbf{v}_F \cdot \nabla \gamma_n + 2\tilde{\omega} \gamma_n - \eta + \eta \gamma_n^2 = 0, \quad (\text{A1})$$

$$\mathbf{v}_F \cdot \nabla \gamma_s + 2\omega \gamma_s - \Delta_k + \Delta_k^* \gamma_s^2 = 0, \quad (\text{A2})$$

with

$$\tilde{\omega} = \omega_n + \frac{\text{Re}(g)}{2\tau_0}, \quad \eta = \frac{\langle f \rangle}{2\tau_0}, \quad \underline{\eta} = -\frac{\langle f \rangle^*}{2\tau_0}. \quad (\text{A3})$$

At the interface,  $\gamma$  can be obtained

$$\gamma_n = -\frac{1}{\underline{\eta}} [\tilde{\omega} - \sqrt{\tilde{\omega}^2 + \eta \underline{\eta}}], \quad \gamma_s = \frac{\Delta_k}{\omega_n + \Omega_n},$$

$$\underline{\gamma}_n = \frac{1}{\eta} [\tilde{\omega} - \sqrt{\tilde{\omega}^2 + \eta \underline{\eta}}] \quad \underline{\gamma}_s = -\frac{\Delta_k^*}{\omega_n + \Omega_n}, \quad (\text{A4})$$

where  $\Omega_n = \sqrt{\omega_n^2 + |\Delta_k|^2}$ . The normal Green's function, for example, can be obtained from them,

$$g(+k, x=0, i\omega_n) = \frac{1 + \gamma_n \underline{\gamma}_s(k)}{1 - \gamma_n \underline{\gamma}_s(k)}, \quad (\text{A5})$$

$$g(-k, x=0, i\omega_n) = \frac{1 + \gamma_s(-k) \underline{\gamma}_n}{1 - \gamma_s(-k) \underline{\gamma}_n}, \quad (\text{A6})$$

The Green's functions at the surface of a semi-infinite  $p$ -wave SC are calculated from the coherence functions,

$$g_{\text{PW}}(\pm k, x=0, i\omega_n) = \frac{1 + \gamma_s(-k) \underline{\gamma}_s(k)}{1 - \gamma_s(-k) \underline{\gamma}_s(k)}. \quad (\text{A7})$$

Comparing Eqs. (A6) and (A7), we see the similarity. Note that this similarity never appears in the  $d$ -,  $f$ -, and  $g$ -wave SCs because  $\langle f \rangle \ll 1$  in those SCs.

- 
- [1] Y. Maeno, H. Hashimoto, K. Yoshida, S. Nishizaki, T. Fujita, J. G. Bednorz, and F. Lichtenberg, Superconductivity in a layered perovskite without copper, *Nature (London)* **372**, 532 (1994).
- [2] A. P. Mackenzie and Y. Maeno, The superconductivity of  $\text{Sr}_2\text{RuO}_4$  and the physics of spin-triplet pairing, *Rev. Mod. Phys.* **75**, 657 (2003).
- [3] C. Kallin and A. J. Berlinsky, Is  $\text{Sr}_2\text{RuO}_4$  a chiral  $p$ -wave superconductor?, *J. Phys.: Condens. Matter* **21**, 164210 (2009).
- [4] A. P. Mackenzie, T. Scaffidi, C. W. Hicks, and Y. Maeno, Even odder after twenty-three years: The superconducting order parameter puzzle of  $\text{Sr}_2\text{RuO}_4$ , *npj Quantum Mater.* **2**, 40 (2017).
- [5] A. Pustogow, Y. Luo, A. Chronister, Y.-S. Su, D. A. Sokolov, F. Jerzembeck, A. P. Mackenzie, C. W. Hicks, N. Kikugawa, S. Raghu, E. D. Bauer, and S. E. Brown, Constraints on the superconducting order parameter in  $\text{Sr}_2\text{RuO}_4$  from oxygen-17 nuclear magnetic resonance, *Nature (London)* **574**, 72 (2019).
- [6] K. Ishida, M. Manago, and Y. Maeno, Reduction of the  $^{17}\text{O}$  Knight Shift in the Superconducting State and the Heat-up Effect by NMR Pulses on  $\text{Sr}_2\text{RuO}_4$ , *J. Phys. Soc. Jpn.* **89**, 034712 (2020).
- [7] A. Chronister, A. Pustogow, N. Kikugawa, D. A. Sokolov, F. Jerzembeck, C. W. Hicks, A. P. Mackenzie, E. D. Bauer, and S. E. Brown, Evidence for even parity unconventional superconductivity in  $\text{Sr}_2\text{RuO}_4$ , *Proc. Natl. Acad. Sci. U.S.A.* **118**, e2025313118 (2021).
- [8] A. N. Petsch, M. Zhu, M. Enderle, Z. Q. Mao, Y. Maeno, I. I. Mazin, and S. M. Hayden, Reduction of the Spin Susceptibility in the Superconducting State of  $\text{Sr}_2\text{RuO}_4$  Observed by Polarized Neutron Scattering, *Phys. Rev. Lett.* **125**, 217004 (2020).
- [9] T. M. Rice and M. Sigrist,  $\text{Sr}_2\text{RuO}_4$ : An electronic analogue of  $^3\text{He}$ ?, *J. Phys.: Condens. Matter* **7**, L643 (1995).
- [10] H. G. Suh, H. Menke, P. M. R. Brydon, C. Timm, A. Ramires, and D. F. Agterberg, Stabilizing even-parity chiral superconductivity in  $\text{Sr}_2\text{RuO}_4$ , *Phys. Rev. Res.* **2**, 032023(R) (2020).
- [11] Y. Fukaya, T. Hashimoto, M. Sato, Y. Tanaka and Y. Tanaka, Spin susceptibility for orbital-singlet Cooper pair in the three-

- dimensional  $\text{Sr}_2\text{RuO}_4$  superconductor, *Phys. Rev. Res.* **4**, 013135 (2022).
- [12] S. Benhabib, C. Lupien, I. Paul, L. Berges, M. Dion, M. Nardone, A. Zitouni, Z. Q. Mao, Y. Maeno, A. Georges, L. Taillefer, and C. Proust, Ultrasound evidence for a two-component superconducting order parameter in  $\text{Sr}_2\text{RuO}_4$ , *Nat. Phys.* **17**, 194 (2021).
- [13] S. Ghosh, A. Shekhter, F. Jerzembeck, N. Kikugawa, D. A. Sokolov, M. Brando, A. P. Mackenzie, C. W. Hicks, and B. J. Ramshaw, Thermodynamic evidence for a two-component superconducting order parameter in  $\text{Sr}_2\text{RuO}_4$ , *Nat. Phys.* **17**, 199 (2021).
- [14] V. Grinenko, S. Ghosh, R. Sarkar, J.-C. Orain, A. Nikitin, M. Elender, D. Das, Z. Guguchia, F. Brückner, M. E. Barber, J. Park, N. Kikugawa, D. A. Sokolov, J. S. Bobowski, T. Miyoshi, Y. Maeno, A. P. Mackenzie, H. Luetkens, C. W. Hicks, and H.-H. Klauss, Split superconducting and time-reversal symmetry-breaking transitions in  $\text{Sr}_2\text{RuO}_4$  under stress, *Nat. Phys.* **17**, 748 (2021).
- [15] V. Grinenko, D. Das, R. Gupta, B. Zinkl, N. Kikugawa, Y. Maeno, C. W. Hicks, H.-H. Klauss, M. Sigrist, and R. Khasanov, Unsplit superconducting and time reversal symmetry breaking transitions in  $\text{Sr}_2\text{RuO}_4$  under hydrostatic pressure and disorder, *Nat. Commun.* **12**, 3920 (2021).
- [16] S. Kobayashi, Y. Tanaka, and M. Sato, Fragile surface zero-energy flat bands in three-dimensional chiral superconductors, *Phys. Rev. B* **92**, 214514 (2015).
- [17] S. Tamura, S. Kobayashi, L. Bo, and Y. Tanaka, Theory of surface Andreev bound states and tunneling spectroscopy in three-dimensional chiral superconductors, *Phys. Rev. B* **95**, 104511 (2017).
- [18] S.-I. Suzuki, M. Sato, and Y. Tanaka, Identifying possible pairing states in  $\text{Sr}_2\text{RuO}_4$  by tunneling spectroscopy, *Phys. Rev. B* **101**, 054505 (2020).
- [19] S. Ikegaya, S.-I. Suzuki, Y. Tanaka, and D. Manske, Proposal for identifying possible even-parity superconducting states in  $\text{Sr}_2\text{RuO}_4$  using planar tunneling spectroscopy, *Phys. Rev. Res.* **3**, L032062 (2021).
- [20] P. G. Björnsson, Y. Maeno, M. E. Huber, and K. A. Moler, Scanning magnetic imaging of  $\text{Sr}_2\text{RuO}_4$ , *Phys. Rev. B* **72**, 012504 (2005).
- [21] J. R. Kirtley, C. Kallin, C. W. Hicks, E.-A. Kim, Y. Liu, K. A. Moler, Y. Maeno, and K. D. Nelson, Upper limit on spontaneous supercurrents in  $\text{Sr}_2\text{RuO}_4$ , *Phys. Rev. B* **76**, 014526 (2007).
- [22] M. Matsumoto and M. Sigrist, Quasiparticle states near the surface and the domain wall in a  $p_x \pm ip_y$ -wave superconductor, *J. Phys. Soc. Jpn.* **68**, 994 (1999).
- [23] A. Furusaki, M. Matsumoto and M. Sigrist, Spontaneous Hall effect in a chiral  $p$ -wave superconductor, *Phys. Rev. B* **64**, 054514 (2001).
- [24] M. Stone and R. Roy, Edge modes, edge currents, and gauge invariance in  $p_x + ip_y$  superfluids and superconductors, *Phys. Rev. B* **69**, 184511 (2004).
- [25] Y. Nagato, S. Higashitani, and K. Nagai, Subgap in the Edge States of Two-Dimensional Chiral Superconductor with Rough Surface, *J. Phys. Soc. Jpn.* **80**, 113706 (2011).
- [26] S. V. Bakurskiy, A. A. Golubov, M. Yu. Kupriyanov, K. Yada, and Y. Tanaka, Anomalous surface states at interfaces in  $p$ -wave superconductors, *Phys. Rev. B* **90**, 064513 (2014).
- [27] S.-I. Suzuki and Y. Asano, Spontaneous edge current in a small chiral superconductor with a rough surface, *Phys. Rev. B* **94**, 155302 (2016).
- [28] S. V. Bakurskiy, N. V. Klenov, I. I. Soloviev, M. Yu. Kupriyanov, and A. A. Golubov, Observability of surface currents in  $p$ -wave superconductors, *Supercond. Sci. Technol.* **30**, 044005 (2017).
- [29] H. Suderow, V. Crespo, I. Guillamon, S. Vieira, F. Servant, P. Lejay, J. P. Brison, and J. Flouquet, A nodeless superconducting gap in  $\text{Sr}_2\text{RuO}_4$  from tunneling spectroscopy, *New J. Phys.* **11**, 093004 (2009).
- [30] I. A. Firmo, S. Lederer, C. Lupien, A. P. Mackenzie, J. C. Davis, and S. A. Kivelson, Evidence from tunneling spectroscopy for a quasi-one-dimensional origin of superconductivity in  $\text{Sr}_2\text{RuO}_4$ , *Phys. Rev. B* **88**, 134521 (2013).
- [31] R. Sharma, S. D. Edkins, Z. Wang, A. Kostin, C. Sow, Y. Maeno, A. P. Mackenzie, J. C. S. Davis, and V. Madhavan, Momentum-resolved superconducting energy gaps of  $\text{Sr}_2\text{RuO}_4$  from quasiparticle interference imaging, *Proc. Natl. Acad. Sci. USA* **117**, 5222 (2020).
- [32] G. Eilenberger, Transformation of Gorkovs equation for type II superconductors into transport-like equations, *Z. Phys. A: Hadrons Nucl.* **214**, 195 (1968).
- [33] The quasiclassical approximation is valid in the weak-coupling limit: The superconducting gap is much smaller than the Fermi energy. This condition is fulfilled in most of the low-temperature superconductors (e.g., BCS-type SC, heavy-fermion compounds, and  $\text{Sr}_2\text{RuO}_4$ )
- [34] N. Schopohl and K. Maki, Quasiparticle spectrum around a vortex line in a  $d$ -wave superconductor, *Phys. Rev. B* **52**, 490 (1995).
- [35] M. Eschrig, Distribution functions in nonequilibrium theory of superconductivity and Andreev spectroscopy in unconventional superconductors, *Phys. Rev. B* **61**, 9061 (2000).
- [36] M. Eschrig, Scattering problem in nonequilibrium quasiclassical theory of metals and superconductors: General boundary conditions and applications, *Phys. Rev. B* **80**, 134511 (2009).
- [37] We have confirmed the similar fragility of the CSC in the  $(f + if')$ -wave SC with  $\Delta_k \sim (\Delta_1 k_x + i\Delta_2 k_y)(5k_z^2 - 1)$ .
- [38] Y. Tanaka, Y. Tanuma, and A. A. Golubov, Odd-frequency pairing in normal-metal/superconductor junctions, *Phys. Rev. B* **76**, 054522 (2007).
- [39] J. Hara and K. Nagai, A Polar State in a Slab as a Soluble Model of  $p$ -Wave Fermi Superfluid in Finite Geometry, *Prog. Theor. Phys.* **76**, 1237 (1986).
- [40] M. Diez, J. P. Dahlhaus, M. Wimmer, and C. W. J. Beenakker, *Phys. Rev. B* **86**, 094501 (2012).
- [41] S.-I. Suzuki and Y. Asano, Effects of surface roughness on the paramagnetic response of small unconventional superconductors, *Phys. Rev. B* **91**, 214510 (2015).
- [42] S. Ikegaya, S.-I. Suzuki, Y. Tanaka, and Y. Asano, Quantization of conductance minimum and index theorem, *Phys. Rev. B* **94**, 054512 (2016).
- [43] S. Kashiwaya, K. Saitoh, H. Kashiwaya, M. Koyanagi, M. Sato, K. Yada, Y. Tanaka, and Y. Maeno, Time-reversal invariant superconductivity of  $\text{Sr}_2\text{RuO}_4$  revealed by Josephson effects, *Phys. Rev. B* **100**, 094530 (2019).
- [44] J. Xia, Y. Maeno, P. T. Beyersdorf, M. M. Fejer, and A. Kapitulnik, High Resolution Polar Kerr Effect Measurements of  $\text{Sr}_2\text{RuO}_4$ : Evidence for Broken Time-Reversal Symmetry

- in the Superconducting State, *Phys. Rev. Lett.* **97**, 167002 (2006).
- [45] Y.-S. Li, N. Kikugawa, D. A. Sokolov, F. Jerzembeck, A. S. Gibbs, Y. Maeno, C. W. Hicks, J. Schmalian, M. Nicklas, and A. P. Mackenzie, High-sensitivity heat-capacity measurements on  $\text{Sr}_2\text{RuO}_4$  under uniaxial pressure, *Proc. Natl. Acad. Sci. USA* **118**, e2020492118 (2021).
- [46] In the two-component model  $\Delta \sim \Delta_1 + i\Delta_2$ , the material shows superconductivity when either of the component is finite ( $\Delta_1 \neq 0$  or  $\Delta_2 \neq 0$ ), whereas the TRS breaking occurs when both components are finite ( $\Delta_1 \neq 0$  and  $\Delta_2 \neq 0$ ). Theoretically, a strain can shift the superconducting transition temperatures in different ways (e.g.,  $T_{c1} > T_{c2}$ ). Namely, under a strain, we expect the temperature range where the material exhibits superconductivity but not TRS breaking (i.e.,  $T_{c2} < T < T_{c1}$ ). However, the experiment reported the temperatures for the superconducting transition temperatures and TRS breaking are identical (i.e.,  $T_{c1} = T_{c2}$ ). This result is incompatible with the  $(d + id')$ -wave model.
- [47] R. Fittipaldi, R. Hartmann, M. T. Mercaldo, S. Komori, A. Bjørli, W. Kyung, Y. Yasui, T. Miyoshi, L. A. B. Olde Olthof, C. M. Palomares Garcia, V. Granata, I. Keren, W. Higemoto, A. Suter, T. Prokscha, A. Romano, C. Noce, C. Kim, Y. Maeno, E. Scheer, B. Kalisky, J. W. A. Robinson, M. Cuoco *et al.* Unveiling unconventional magnetism at the surface of  $\text{Sr}_2\text{RuO}_4$ , *Nat. Commun.* **12**, 5792 (2021).